Soft Matter

Accepted Manuscript

ROYAL SOCIETY OF CHEMISTRY

www.rsc.org/softmatter

Table of Contents graphics

Designing Lipids for Selective Partitioning Into Liquid Ordered Membrane Domains

Noor Momin, Stacey Lee, Avinash Gadok, David J. Busch, George D. Bachand, Carl C. Hayden, Jeanne C. Stachowiak, and Darryl Y. Sasaki

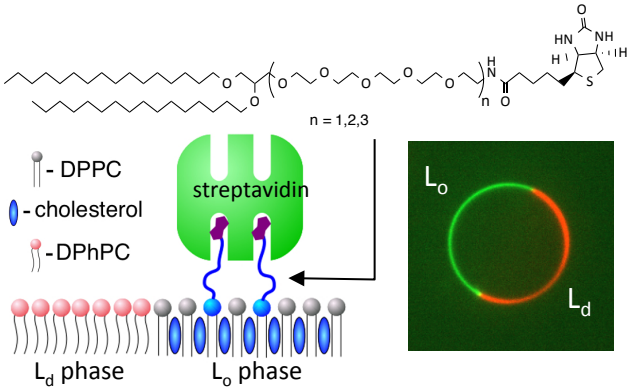

Short PEG spacers effectively decouple headgroup and receptor-ligand interactions from the membrane allowing packing order of the lipid tails to direct partitioning of lipids to specific membrane phases.

Designing Lipids for Selective Partitioning Into Liquid Ordered Membrane Domains

Noor Momin[†£], Stacey Lee[†¶], Avinash K. Gadok[£], David J. Busch[£], George D. Bachand[§], Carl C. Hayden[‡], Jeanne C. Stachowiak[£], and Darryl Y. Sasaki[†*]

Sandia National Laboratories, [†]Biotechnology and Bioengineering Dept. and [‡]Combustion Chemistry Dept., Livermore, CA and [§]Nanosystems Synthesis/Analysis Dept., Albuquerque, NM

[£]The University of Texas at Austin, Department of Biomedical Engineering

Abstract

Self-organization of lipid molecules into specific membrane phases is key to the development of hierarchical molecular assemblies that mimic cellular structures. While the packing interaction of the lipid tails should provide the major driving force to direct lipid partitioning to ordered or disordered membrane domains, numerous examples show that the headgroup and spacer play important but undefined roles. We report here the development of several new biotinylated lipids that examine the role of spacer chemistry and structure on membrane phase partitioning. The new lipids were prepared with varying lengths of low molecular weight polyethylene glycol (EGn) spacers to examine how spacer hydrophilicity and length influence their partitioning behavior following binding with FITC-labeled streptavidin in liquid ordered (L_o) and liquid disordered (L_d) phase coexisting membranes. Partitioning coefficients ($K_{p\ Lo/Ld}$) of the biotinylated lipids were determined using fluorescence measurements in studies with giant unilamellar vesicles (GUVs). Compared against DPPE-

biotin, DPPE-cap-biotin, and DSPE-PEG2000-biotin lipids, the new dipalmityl-EGn-biotin lipids exhibited markedly enhanced partitioning into liquid ordered domains, achieving K_p of up to 7.3 with a decaethylene glycol spacer (DP-EG10-biotin). We further demonstrated biological relevance of the lipids with selective partitioning to lipid raft-like domains observed in giant plasma membrane vesicles (GPMVs) derived from mammalian cells. Our results found that the spacer group not only plays a pivotal role for designing lipids with phase selectivity but may also influence the structural order of the domain assemblies.

Introduction

The cell membrane is a heterogeneous assembly of lipids and proteins that organize into microdomain architectures for specific cellular tasks,[1] such as signaling[2] and trafficking,[3] as well as being sites for pathogen entry.[4] Some of these organized molecular assemblies form phases of high structural order with physical and mechanical properties that are distinct from the rest of the fluid membrane.[5,6] These domain architectures, also known as lipid rafts, [7,8] are believed to provide a basis for understanding cellular physiology and insight into membrane structure transformation through lipid sorting and protein-membrane interaction.[9,10] Being able to target these molecular assemblies, either through lipidic moieties within the membrane or from ligands sequestered from bulk solution, would make it possible to develop probes to track the formation and transport of membrane microdomains. However, the design rules for building such lipids is incomplete.[11,12,13]

Model systems provide a platform for studying partitioning behavior and dynamics of membrane assemblies under controlled conditions. Some features of lipid raft-like structures in membranes can be replicated using a ternary system composed of (1) a lipid with long, straight-chain saturated hydrocarbon tails that facilitates high packing order (distinguished by a high phase transition temperature (T_m)), (2) another lipid of low packing order (low T_m), and (3) a sterol, such as cholesterol, to generate coexisting regions of liquid ordered (L_o) and liquid disordered (L_d) membrane phases.[14] Selective labeling of these phases with lipids and proteins provides a means to probe the physical and mechanical properties of membrane domains.

Proteins and other ligands can be readily coupled to lipid membranes through the biotin-streptavidin interaction.[15] This strategy has been used in a variety of sensing[16] and characterization[17] techniques on lipid membranes as well as a route towards cell surface

engineering.[18] Studies to understand the phase partitioning of commercially available biotin-lipids, however, have found that they prefer the disordered L_d phase even when lipid structure would suggest preferential partitioning to the raft-like L_o phase. For example, the partitioning coefficient for DPPE-cap-biotin with long saturated hydrocarbon tails that are expected to prefer regions of high packing order instead exhibits a strong preference for the disordered phase ($K_{p\ Lo/Ld} \sim 0.2$).[19,20] In a profound example of the effect of spacer chemistry on lipid phase partitioning, Wang et al.[21] showed that by replacing the cap spacer with PEG1450, DSPE-PEG1450-biotin effectively sequesters streptavidin to liquid ordered domains in Jurkat cells. A PEG spacer was also found to switch the partitioning behavior of the fluorophore-labeled lipid DSPE-KK114 from selectivity towards the L_d phase ($K_p < 0.1$) to the L_o phase ($K_p = 2.5$) with DSPE-PEG1450-KK114.[22]

The ability of the PEG spacer to dramatically alter phase partitioning behavior provides valuable insight into lipid structure design. PEG is a unique material that strongly complexes water but also enables solubilization of non-polar substrates.[23] Due to its biocompatibility and ability to impart aggregation resistance to liposomes and proteins it has been employed by the pharmaceutical industry for improving circulation times of drug delivery systems.[23] Despite these attributes, PEGylated lipids are also known to disrupt membrane structure causing leakage of entrapped material,[24] loss of film planarity,[25,26] and phase separation from ordered lipid regions.[27,28] Such observations are especially true of lipids with high molecular weight PEG that impart large spontaneous curvature. These lipids readily form micellar structures in water and when incorporated into lipid vesicles their mole fraction must be kept low (e.g., < 8% for PEG2000) in order to maintain vesicle structure.[29] Small molecular weight PEGylated lipids, on

the other hand, are not known to disrupt membrane structure and can serve as steric barriers to resist protein adhesion,[30] but have limited utility for enhancing blood circulation times.[31]

It is evident from past results that spacer chemistry plays an influential role in lipid partitioning behavior. While a hydrophobic caproyl spacer can usher a lipid with long straight-chain hydrocarbon tails towards the L_d phase, a hydrophilic PEG spacer can reverse the behavior allowing the lipid tails to direct the phase miscibility. However, since long PEG spacers may prove detrimental for membrane structure/stability, further understanding of the role of spacer chemistry and structure in lipid phase partitioning is needed. In past work we have shown that ether-linked glycero-lipids with palmityl tails and iminodiacetic acid (IDA) headgroup partition into the ordered lipid membrane phase.[32] This partitioning enabled selective affinity of his-tagged proteins to gel-phase and liquid ordered domains via the Cu(II)-IDA complex. A feature of these lipids is a triethylene glycol spacer, which provides a hydrophilic tether that can extend the IDA headgroup several angstroms away from the membrane surface.[33] Using this simple lipid design as a starting point we prepared a series of biotin-functionalized lipids with varying lengths of low molecular weight PEG spacers in an effort to identify optimal spacer chemistry and structure for selective phase partitioning (Figure 1). We report on the general characteristics of the lipid (T_m, Langmuir monolayer isotherms) and their phase partitioning behavior in giant unilamellar vesicles (GUVs) and giant plasma membrane vesicles (GPMVs) with FITC-streptavidin.

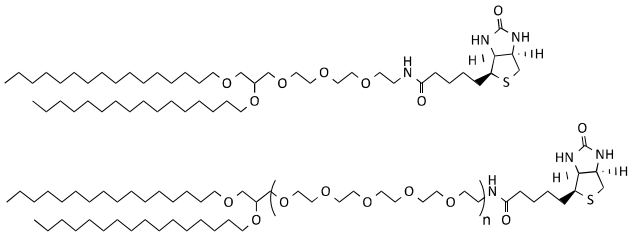

Figure 1. Lipid structures for DP-EG3-biotin (top) and DP-EG5-biotin (where n = 1), DP-EG10-biotin (n = 2), and DP-EG15-biotin (n = 3).

Experimental Section

General

Aqueous solutions were prepared from deionized water obtained through a Barnstead Type D4700 NANOpure Analytical Deionization System with ORGANICfree cartridge registering ≥ 18.0 MΩ-cm resistance. DPPE-biotin, DOPE-biotin, DPPE-cap-biotin, and DOPE-cap-biotin lipids were purchased from Avanti Polar Lipids (Alabaster, AL). All solvents and reagents were purchased from either Fisher Scientific (Pittsburg, PA) or Sigma-Aldrich (St. Louis, MO) unless otherwise stated. ^{1}H (500 MHz) and ^{13}C NMR (125 MHz) spectra were taken on a Varian INOVA 500. Infrared spectra were taken on a Nicolet Avatar 360 FT-IR. Elemental analysis was performed by Columbia Analytical Services (Tucson, AZ). Chinese hamster ovary (CHO) cells were obtained from American Type Culture Collection (Manassas, VA).

Lipid synthesis

Procedures for preparing and the spectroscopic data of DP-EG3-biotin, DP-EG5-biotin, DP-EG10-biotin, and DP-EG15-biotin can be found in the Supporting Information.

Differential scanning calorimetry

DSC measurements of hydrated lipid films were taken on a Mettler Toledo HP DSC1 (Columbus, OH). In brief, 8-9 mg of lipid was dissolved in 1 mL of chloroform, or in the case of DPPE-cap-biotin 50% methanol/chloroform, and evaporated as a thin film onto the wall of a glass conical vial using a rotary evaporator. The films were further dried under vacuum overnight, followed by hydration with ~150 μL of water at ~50 °C and vortex stirring.

Approximately 70 μL of the film solution was then transferred to an aluminum crucible, weighed, and the measurement run from 10 – 80 °C at a heating rate of 2 °C/min. All data are shown in Figure S1 and the phase transition temperatures (T_m) presented in Table 1.

Langmuir film studies

All Langmuir monolayer π-A isotherms were performed on a KSV Minitrough (Helsinki, FI). The aqueous subphase temperature was maintained with ± 0.1 ^oC accuracy using a Neslab RTE-101 water circulator. Lipids were spread either on pure water from chloroform solution or, in the case of DPPE-cap-biotin, from a 50% methanol/chloroform solution. Following spreading the surface was allowed to incubate for 10 – 15 minutes prior to compression. The compression rate for π-A isotherms was 37.5 cm^2/min (~5 $Å^2$/molecule•min).

GUV preparation

Giant unilamellar vesicles were prepared by electroformation following published procedures.[34] All vesicles were prepared at an elevated temperature that exceeded the highest phase transition temperature of the lipid mixtures (e.g., for samples containing DPPC the GUVs were prepared at 55 – 60 °C) and contained 0.3 mol% of a red fluorescent-labeled lipid (either TRITC-DHPE or BODIPY 530/550 HPC) to identify the L_d phase. Vesicles were initially prepared in sucrose solution (~350 mOsm) and following electroformation the vesicles were diluted in MOPS buffer (20 mM 3-(N-morpholino) propanesulfonic acid, pH 7.4, adjusted to 350 mOsm with NaCl [~ 0.16 M]).

Determination of partition coefficients

Freshly formed GUVs were combined with a stock solution of FITC-streptavidin (Invitrogen) in MOPS buffer solution to yield a final solution concentration of 1 μM of the protein. The mixture was then placed in a channel structure constructed of a glass coverslip and slide sandwiching parallel strips of double-sided tape (3 layers thick) spaced 2 – 3 mm apart. The ends of the fluidic structure were then sealed with wax to minimize evaporation and imaged within five minutes to ensure sample freshness. Images were captured in epifluorescence (Figures 4 A and B, S3, S4, S6, S7, S9, and S10) using a Zeiss Axiovert 200M microscope with a Sutter Lambda XL broadband light source under green (filter set of λ_{ex} = 472 nm, 30 nm bandpass; λ_{em} = 520 nm, 35 nm bandpass) and red channels (filter set of λ_{ex} = 543 nm, 22 nm bandpass; λ_{em} = 593 nm, 40 nm bandpass), or with a Zeiss Axio Observer Z1 with Yokogawa CSU-X1M spinning disk confocal microscope (Figures 3, 4 C and D, 5, and S8) using laser wavelengths of 488 nm (filter set of λ_{em} = 525 nm, 50nm bandpass) and 561 nm (filter set of λ_{em} = 629nm, 62 nm bandpass) with a triple pass dichroic mirror of 405/4 88/561nm.

Partitioning coefficients were determined using the pixel intensities of the images captured in the green channel for FITC-streptavidin. Using the Plot Profile feature on ImageJ, the average pixel intensity along the L_o and L_d domains were determined for each vesicle. Bleed-through from the lipid dye into the protein channel was corrected for using the average phase pixel intensity, under identical imaging conditions, of vesicles in the absence of protein. The low (0.3 mole%) lipid label concentration minimizes potential for FRET based quenching of the FITC-streptavidin. At this concentration the majority of streptavidin molecules do not have a lipid dye label within Förster radius of their center, thus limiting any contribution from FRET quenching in the partition coefficients to an estimated 20% (see SI). No less than 30

measurements taken in random orientations were obtained for each averaged value reported in Table 2.

Giant plasma membrane vesicles

The vesicles were formed following established protocols.[35] In brief, confluent CHO cells in a 75 mL flask were washed twice with 2 mL of GPMV buffer (2 mM $CaCl_2$, 10 mM HEPES, 150 mM NaCl), then once with 2 mL of active buffer (2 mM $CaCl_2$, 10 mM HEPES, 150 mM NaCl, 25 mM paraformaldehyde, 2 mM dithiothreitol), followed by incubation overnight in 3 mL of the active buffer. The active buffer was then collected and the vesicles removed from solution via centrifugation at 17,000g. The pelleted GPMVs were resuspended with GPMV buffer.

Concanavalin A (Sigma-Aldrich), a lectin used to induce membrane phase separation,[36] was labeled with Atto 594-NHS ester (Sigma-Aldrich). FITC-streptavidin was labeled with Atto 488-NHS ester (Sigma-Aldrich) to a ~3:1 ratio to enhance its fluorescence signal. The lipids DP-EG10-biotin and DPPE-cap-biotin were prepared at 1.0 mM stock solutions in tetrahydrofuran (THF).

Biotinylated lipids were added to the GPMV solution from their THF stock solutions to yield a final solution concentration of 100 μM. The solution was mixed thoroughly, then lectin-Atto 594 was added from a 25 μM stock solution to a final solution concentration of 1.25 μM. Following phase separation of the membrane, FITC-streptavidin-Atto 488 was added to the GPMVs at a concentration of 0.8 μM and the vesicles imaged via fluorescence microscopy. Naphthopyrene (Tokyo Chemical Industry) was added to solution (3.75 μM) from DMSO stock solution to label the L_o phase[13] and confirm the partitioning of lectin-Atto 594 to the L_d phase.

Results

Biotinylated lipid properties

The design of our ether-linked biotinylated lipids originates from previous work on a phase partitioning lipid (DPIDA) that facilitated selective binding of his-tagged proteins to L_o phase domains on biphasic GUVs.[32] DP-EG3-biotin is identically structured to DPIDA with the iminodiacetic acid headgroup replaced with biotin. Longer spacers were inserted between the lipid's glycerol backbone and the biotin headgroup by simply appending pentaethylene glycol units to generate DP-EG5-biotin, DP-EG10-biotin, and DP-EG15-biotin. The phase transition temperature (T_m) of the ether-linked biotinylated lipids and the PE-biotin and PE-cap-biotin lipids were measured by DSC (Supporting Information, Figure S1) and the results reported in Table 1. All DP-EGn-biotin lipids have T_m above room temperature but the transition temperature falls as the PEG spacer increases starting from a high of 57 °C for DP-EG3-biotin dropping to a low of 40 °C for DP-EG15-biotin. This inverse relationship between length of the PEG spacer and the lipid's T_m can be understood as a result of increase in steric bulk of the spacer that interferes with the packing order of the lipids. The saturated dipalmitoyl PE lipids, DPPE-biotin and DPPE-cap-biotin, gave T_m's of 34 °C and 32 °C, respectively, indicative of good packing order within the lipid films. However, for DOPE-biotin and DOPE-cap-biotin, with the poor packing order of unsaturated oleoyl lipid tails, their T_m's fell below our measurement range (< 10°C).

Table 1. Phase transition temperatures of biotinylated lipids

Lipid	Phase transition T (°C)[a]
DOPE-biotin	< 10

DOPE-cap-biotin	< 10
DPPE-biotin	34
DPPE-cap-biotin	32
DP-EG3-biotin	57
DP-EG5-biotin	48
DP-EG10-biotin	42
DP-EG15-biotin	40

a) Values obtained from DSC measurements (Figure S1).

Langmuir monolayer isotherms of the DP-EGn-biotin lipids confirm the influence of tail structure and spacer length on packing order. Figure 2 shows that in the condensed phase DP-EG3-biotin and DP-EG5-biotin pack to a molecular area of ca. 40 $Å^2$/molecule, equivalent to the cross section of the two saturated straight-chain hydrocarbon tails. In comparison, DP-EG10-biotin and DP-EG15-biotin gave slightly larger molecular areas (ca. 50 $Å^2$/molecule) confirming the increased role of steric bulk of the spacer at higher PEG molecular weight. Further influence of the PEG spacer length was observed at low surface pressures as the monolayer's expanded phase undergoes a transition similar to the pancake-to-mushroom transition observed with PEGylated lipids.[37] The areas at which pressure was first detected (i.e., "lift off" point) increases as the spacer length increases from 168 $Å^2$/molecule for DP-EG3-biotin to 200 $Å^2$/molecule for DP-EG5-biotin, 410 $Å^2$/molecule for DP-EG10-biotin, and out to 680 $Å^2$/molecule for DP-EG15-biotin. All DP-EGn-biotin lipids exhibit phase coexistence regions between expanded and solid phases but as the spacer length increases the regions exist at increasingly higher pressures and cover a smaller range of molecular area. At membrane related pressures (30 - 35 mN/m),[38] DP-EG3-biotin and DP-EG5-biotin are highly condensed but DP-EG10-biotin and DP-EG15-biotin exhibit signs of increased molecular volume. DPPE-biotin and DPPE-cap-biotin

isotherms are remarkably similar to the DP-EG3-biotin and DP-EG5-biotin lipids (SI, Figure S2) with phase coexistence regions at 14 – 16 mN/m that transition into highly condensed phase at pressures above 20 mN/m and collapse pressure of ca. 58 mN/m. In contrast, the isotherms for the biotinylated DOPE lipids exist primarily in the liquid expanded phase with collapse pressures of ca. 44 mN/m.

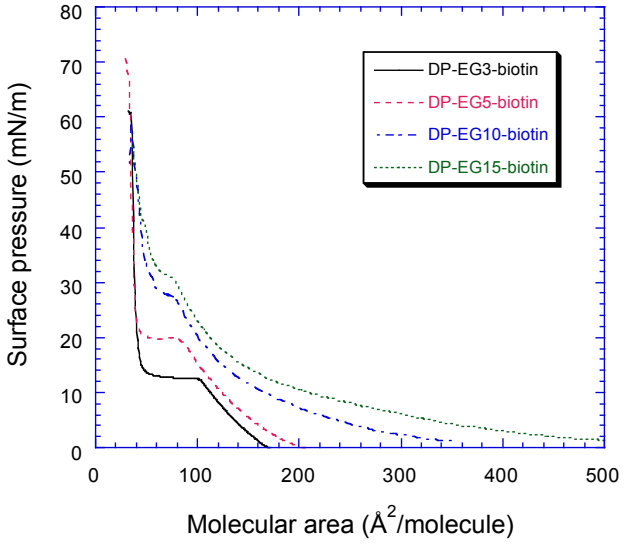

Figure 2. Langmuir monolayer isotherms of DP-EGn-biotin lipids on pure water subphase at 20 °C.

Partitioning behavior of PE-biotin lipids in GUVs

Studies of the partitioning behavior of the biotinylated PE lipids and the new DP-EGn lipids were performed with GUVs of L_o/L_d phase separated membranes. The membranes studied followed compositions described by Veatch, et al.,[39] where the bilayers contain a mixture of DPhPC/DPPC/cholesterol/biotinylated lipid with 0.3% of a red fluorescent lipid (TRITC-DHPE or BODIPY 530/550 HPC) to label the L_d phase. A phase diagram of the ternary lipid mixture is shown in Figure 3. The multicolored area of the phase diagram is the L_o and L_d phase

coexistence region. We used the strong, selective affinity of FITC-streptavidin to the biotinylated lipid to provide optical identification of their phase distribution on the GUVs.

We first conducted studies to confirm the partitioning of the biotinylated PE lipids to the L_d phase as reported by Sarmento et al. [19] and Manley et al.[20] For DPPE-biotin, DPPE-cap-biotin, DOPE-biotin, and DOPE-cap-biotin we indeed observed an affinity of streptavidin for the L_d phase in phase separated GUVs. Examples of phase separated GUVs containing 2 – 11% of DPPE-biotin or DOPE-biotin bound with FITC-streptavidin can be found in the Supporting Information (Figure S3). Fluorescence micrograph images revealed a correspondence of green fluorescence from FITC-streptavidin to the red fluorescence of TRITC-DHPE-labeled L_d regions of the membrane. Similar results were obtained with DPPE-cap-biotin and DOPE-cap-biotin (Figure S4).

At this point we were curious to see if membrane-bound streptavidin might induce in-plane or out-of-plane structural transformations of the domain due to protein crystallization or steric interactions. While it is known that unlabeled streptavidin readily forms 2D crystals on Langmuir films[40] as well as on lipid vesicles,[20] FITC-streptavidin can crystallize on Langmuir films[40] but not vesicles.[20] Irregular shaped domains and sharp edges indicative of 2D streptavidin crystallization[20] were not observed in our studies, instead the FITC-streptavidin-bound domains were circular indicative of a fluid phase. Regarding steric interactions, the membrane bound streptavidin represents a large volume covering an area of ~26 nm^2, [41] equivalent to approximately 30 molecules of DPhPC (~0.8 nm^2)[42] in the L_d phase. Since the nominal mole fraction of biotinylated lipids within the domain can exceed the ratio of 2 biotin lipids bound per streptavidin/30 DPhPC lipids (~7%) it is possible that steric pressure from high protein loading could induce a change in the domain structure.[43] We did not observe any signs

of large scale deformation, such as tubules or budded vesicles from the GUVs, that would be indicative of induced membrane curvature from asymmetric steric pressure from the externally bound proteins on the lipid domains. Regarding the expansion or dissolution of membrane domains due to lateral pressure from bound proteins within the domains,[44] we measured domain size in GUVs before and after exposure to streptavidin. Different membrane compositions of DPhPC/cholesterol/DPPC, containing biotinylated PE lipid at low (~10% biotin lipid/DPhPC) and high (~25% biotin lipid/DPhPC) concentration, were examined. By selecting only images where the L_o and L_d phases were 1) clearly separated into two distinct domains, and 2) oriented such that their mid-section coincided with vesicle's equator, we could calculate the domain size (Figure S5). We found no change in average domain size following streptavidin binding at all membrane compositions and biotinylated PE lipids used.

Partitioning behavior of DP-EG$_n$-biotin lipids in GUVs

Next, we examined the phase partitioning behavior of the DP-EGn-biotin lipids. From the phase diagram[39] of Figure 3 we selected several lipid compositions representing different miscibility transition temperatures (T_{MT}) regions of the L_o/L_d phase coexistence. The miscibility transition temperature (color scale below the phase diagram) is the temperature at which the biphasic membrane transitions into a single phase. Higher T_{MT}, which increases with mole fraction of DPPC, suggests improved packing order of the L_o phase. GUVs were composed of DPhPC/DPPC/cholesterol/DP-EGn-biotin (with 0.3% BODIPY 530/550 HPC to label the L_d phase) at the corresponding molar ratios of (A) 56:17:25:2, (B) 28:25:44:3, (C) 38:34:24:4, and (D) 20:43:32:5. Figure 3 shows images of GUVs containing DP-EG10-biotin at these four membrane compositions following exposure to FITC-streptavidin. The percentage of the

biotinylated lipid at all the membrane compositions was maintained at ~10% of the mole fraction of C16 lipids (i.e., DPPC and DP-EGn-biotin) in the membrane. The fluorescence images of Figure 3 show high selective affinity of FITC-streptavidin to the L_o phase with bilayers containing DP-EG10-biotin at all membrane compositions. Images of the other DP-EGn-biotin lipids and DSPE-PEG2000-biotin in GUVs at membrane compositions A-D are shown in the Supporting Information (Figures S6 – S9).

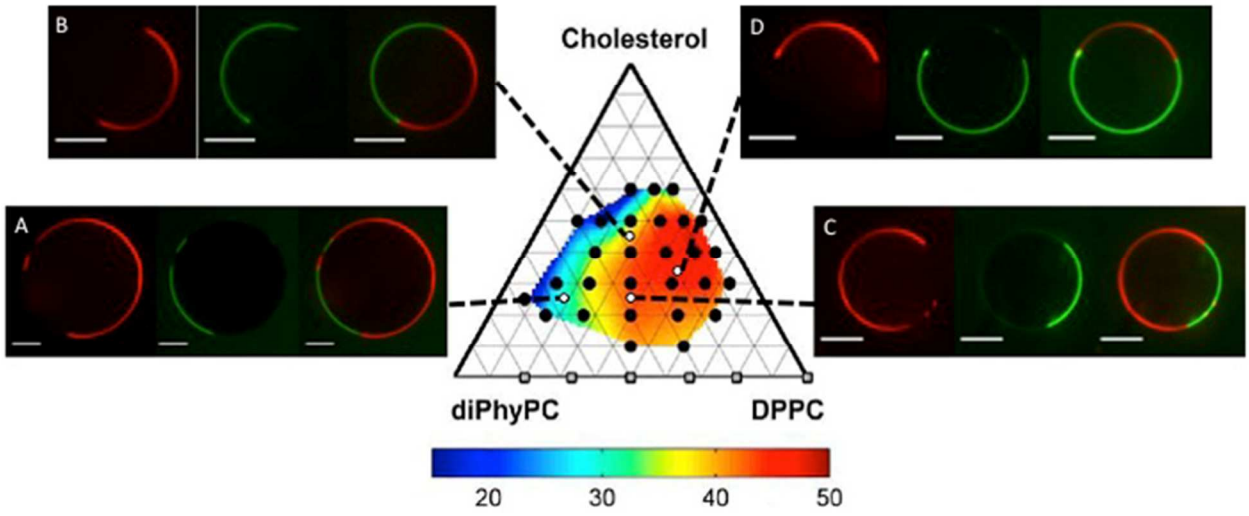

Figure 3. Fluorescence images of DP-EG10-biotin-containing GUVs showing the selective affinity of FITC-streptavidin (green) to the L_o phase contrasted against the L_d phase (red). Several membrane compositions were examined and representative images of the GUVs are shown along with the merged images. GUVs composed of DPhPC/DPPC/cholesterol/DP-EG10-biotin/BODIPY 530/550 HPC at corresponding ratios of: (A) 56:17:25:2:0.3, (B) 28:25:44:3:0.3, (C) 38:34:24:4:0.3, (D) 20:43:32:5:0.3. All solutions contained 1 μM FITC-streptavidin. Phase diagram image is from reference 42. Scale bars are 10 μm.

Figure 4 shows representative images of GUVs with membrane composition A containing each of the DP-EGn-biotin lipids following exposure to FITC-streptavidin. From these images a general trend can be observed in which an increase in spacer length (n) results in enhanced partitioning to the L_o phase. Partition coefficients (K_p) were determined from the images using the fluorescence intensity of the membrane bound FITC-streptavidin (Figure S10).

Assuming similar fluorescence lifetimes of the FITC-labeled streptavidin on both the L_o and L_d phases,[19] K_p could be simply determined as I_{Lo}/I_{Ld}, where I_{Lo} is the fluorescence intensity from the L_o phase and I_{Ld} is the intensity from the L_d phase from the green channel. The K_p values are shown in Table 2.

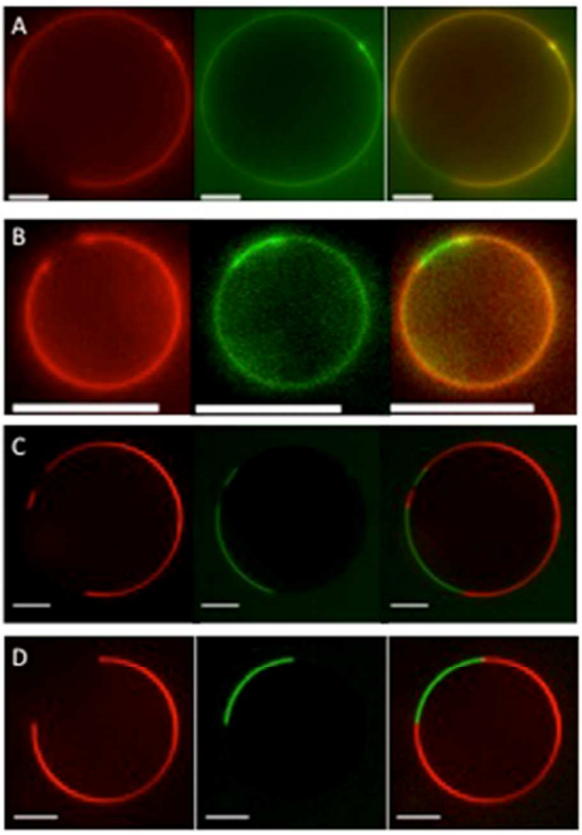

Figure 4. Enhancement of FITC-streptavidin selective affinity to L_o phase in phase separated GUVs with increasing spacer length in DP-EGn-biotin lipids. Fluorescence microscopic images of GUVs composed of 56% DPhPC /25% Cholesterol /17% DPPC/0.3% BODIPY 530/550 HPC (composition A in Table 2) with 2% of (a) DP-EG3-biotin,(b) DP-EG5-biotin, (c) DP-EG10-biotin, and (d) DP-EG15-biotin, incubated with 1 μM FITC-streptavidin. Images taken in the red channel (left) shows the BODIPY 530/550 HPC labeled L_d phase, the green channel (middle) shows FITC-streptavidin, and on the right are the merged images. Scale bars are 10 μm.

It is interesting to observe that as the PEG chain increases in length from 3 to 10 the partition coefficient improves rather dramatically from equal partitioning for either phase with DP-EG3-biotin to a 7:1 selectivity of L_o to L_d phase for DP-EG10-biotin at membrane composition C. As the PEG length goes beyond EG10, however, the partition coefficients tend to decrease, as is

seen with the 15-mer (equivalent to PEG660) and PEG2000. Another trend worth noting is that the DP-EGn-biotin lipids exhibit higher K_p values in membranes compositions with increasing T_{MT}, whereas with DSPE-PEG2000-biotin the K_p values increase with decreasing T_{MT}. The trend suggests that DP-EGn-biotin lipids prefer membrane phases of high packing order, whereas DSPE-PEG2000-biotin prefers lower packing order within an L_o phase.

Table 2. Partition coefficient K_p (L_o/L_d) of biotinylated lipids in DPhPC/DPPC/cholesterol membranes[a]

Biotin lipid	A	B	C	D
DP-EG3-biotin	0.9 (± 0.2)	1.0 (± 0.2)	1.0 (± 0.1)	0.9 (± 0.1)
DP-EG5-biotin	1.2 (± 0.1)	1.2 (± 0.1)	1.1 (± 0.1)	1.1 (± 0.2)
DP-EG10-biotin	2.4 (± 0.7)	4.3 (± 0.9)	7.3 (± 0.9)	5.7 (± 0.9)
DP-EG15-biotin	2.5 (± 0.5)	2.8 (± 0.7)	4.0 (± 1.0)	3.9 (± 1.2)
DSPE-PEG2000-biotin	1.8 (± 0.4)	1.7 (± 0.2)	1.3 (± 0.2)	1.2 (± 0.2)

a) Membrane compositions A- D described in text. Standard deviations of K_p values shown in parentheses.

Role of spacer size

Steric size of the spacer could play a role in some of the trends observed in K_p. The cross sectional area of PEG2000 on the membrane surface can be approximated using the Flory radius $R_F = \square N^{3/5}$, where a is the monomer size (0.35 nm for PEG) and N is the number of monomers (45 for PEG2000)[24] yielding R_F = 3.4 nm and an area of 37 nm^2. Using a molecular area of 0.50 nm^2 for DPPC and 0.27 nm^2 for cholesterol[45] we calculate that for a DPPC-rich L_o domain

PEG2000 would cover ~70 lipids, whereas for a 1:1 DPPC/cholesterol L_o domain PEG2000 would cover ~50 paired couples of DPPC and cholesterol. If we may extend the Flory model to the smaller PEG lengths for DP-EG10-biotin and DP-EG15-biotin, we find R_F of 1.4 nm and 1.8 nm for the EG10 and EG15 lipids, respectively, with corresponding areas of 6.1 nm^2 and 9.9 nm^2. These calculated areas are not to be compared to those measured by the Langmuir isotherms (i.e., lift off areas) since pure PEGylated lipid films at the air-water interface are in a very different solvent environment compared to PEGylated lipids at low density in a bilayer membrane.[46] The areas for the EG10 and EG15 lipids, respectively, equal 12 DPPC molecules or 8 DPPC/cholesterol pairs (~1:10 DP-EG10-biotin/DPPC) and 20 DPPC molecules or 13 DPPC/cholesterol pairs (~1:16 DP-EG15-biotin/DPPC). It must be kept in mind that these are gross estimates since we do not know the influence of biotin on the PEG conformational structure and that the Flory model, designed for large PEG ($N \geq 100$), may not scale well to smaller PEG ($N \leq 20$).[47] However, it is reasonable to consider that as the PEG spacer increases in length there will be less room available per biotinylated lipid within the L_o domain.

Considering the ratio of lipids per PEG2000 in a given area and knowing that the mushroom-to-brush transition occurs at around 4% of PEG2000 in a PC membrane,[24,48] reducing the amount of DSPE-PEG2000-biotin by several-fold from the nominal concentration of 10 mole% should reduce steric congestion and improve selectivity for the L_o phase. Similarly for DP-EG15-biotin, where the nominal mole fraction of biotin lipid/DPPC exceeds the steric volume available with the L_o domain, improvement in selective partitioning should also be observed. However, for DP-EG10-biotin where the nominal mole fraction nearly matches the steric volume available within the L_o domain, there should be little observed change in partitioning behavior.

We reduced the amount of biotinylated lipid five-fold in membrane composition C (0.8 mole %) and observed that the selectivity for DP-EG15-biotin ($K_p = 6.3 \pm 1.2$) does indeed improve matching that of DP-EG10-biotin ($K_p = 6.6 \pm 1.3$) (images in Figure S11). This level of selectivity is a significant improvement compared to the results shown in Table 2 at membrane composition C with 4 mole % of biotinylated lipid where DP-EG10-biotin has a 1.8 times greater coefficient than DP-EG15-biotin. We also observed that DSPE-PEG2000-biotin partitioned well to L_o domains in some GUVs, however, the partitioning behavior was not consistent amongst the vesicles. A common observation was the presence of regions rich in streptavidin but forming in the absence of a distinct corresponding L_o phase in the membrane (Figure S11E).

Phase Partitioning in GPMVs

To assess the physiological relevance of the observed phase partitioning we also conducted studies with giant plasma membrane vesicles (GPMVs). Biotinylated lipids were incorporated into the membranes and the affinity of fluorescent-labeled streptavidin to L_o (raft-like) or L_d (non-raft) domains was evaluated. GPMVs were isolated from CHO cells and then exposed to Atto-594 labeled concanavalin A (lectin) to induce membrane phase separation of the vesicles.[36] Napthopyrene was added to solution to label the liquid ordered phase of the GPMVs.[13] Figure 5 (B and C) shows confocal fluorescence images where the lectin (red channel) and naphthopyrene (green channel) partition to distinctly separate regions suggesting that the lectin is concentrated in the L_d phase. The scale of phase separation varied significantly over the population of vesicles, such that some vesicles had many small domains (Figure 5B and D) while others yielded a few large domains (Figure 5C and E). With the addition of DP-EG10-biotin to the phase separated vesicles we observed selective affinity of fluorescent-labeled

streptavidin to the raft-like L_o phase (Figure 5D). In contrast, when DPPE-cap-biotin was added to vesicles we found that the streptavidin selectively bound to the L_d phase (Figure 5E). These results confirmed the physiological relevance of the phase partitioning we observed with the model membrane studies.

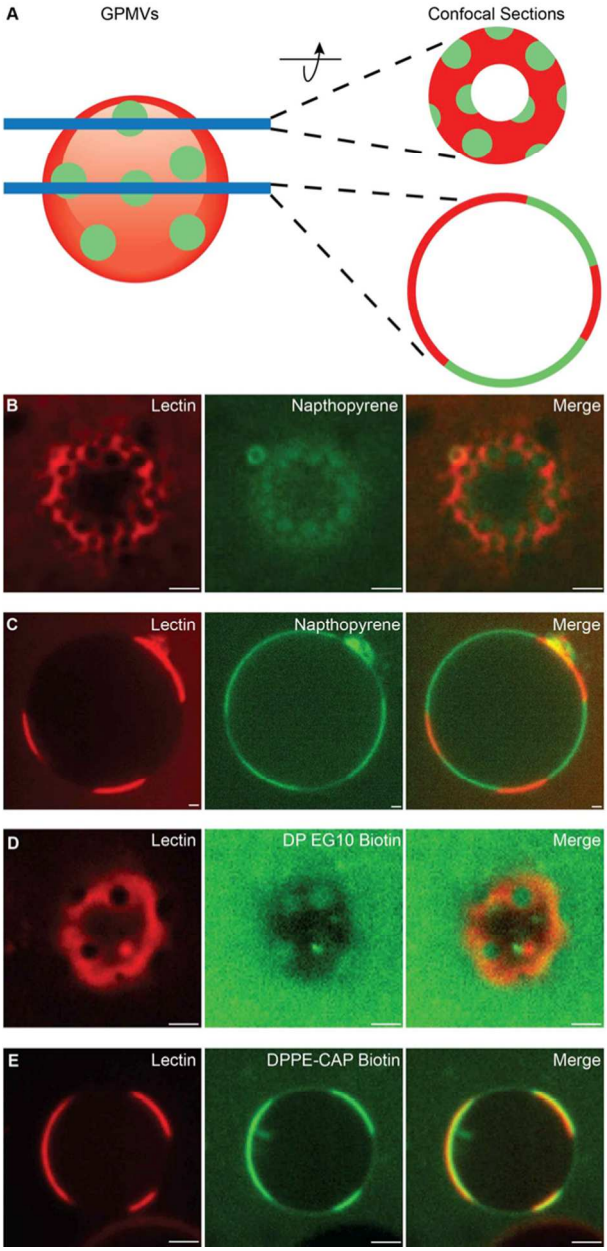

Figure 5. Selective partitioning of proteins and lipids into L_d and L_o phases in cell derived GPMVs. (A) Side view of a diagram demonstrating that a spherical GPMV (left) may appear differently depending on where a confocal section (blue lines) is acquired. The image of a confocal section acquired through the top of a spherical GPMV will appear as an annulus (top right), however, a confocal section through the equator of a spherical GPMV will appear as a large circle (bottom right). (B-C) Atto-594-lectin (red) drives both large and small-scale phase separation in GPMVs with preferential affinity to the L_d phase, while

naphthopyrene (green) partitions to the L_o phase. (D) Atto-488-FITC-streptavidin (green) selectively binds to L_o phase when DP-EG10-biotin is present, but (E) binds to the L_d phase when DPPE-cap-biotin is present. Scale bars are 2 μm.

Discussion

One of the most important findings from our results is that by simply changing the chemistry of the spacer the partitioning behavior of biotinylated lipids can change dramatically. If we compare DP-EG5-biotin with DPPE-cap-biotin, both of which have C16 saturated hydrocarbon tails and nearly the same spacer length between the glycerol backbone and the biotin headgroup, a significant difference in K_p is observed. While DP-EG5-biotin partitions with a slight preference to the L_o phase (K_p = 1.2), DPPE-cap-biotin exhibits predominant partitioning to the L_d phase. Even DP-EG3-biotin, with the shorter PEG spacer length, exhibits equal partitioning K_p (1.0). The inherent high packing order of DPPE-cap-biotin as determined by its phase transition temperature and Langmuir isotherm behavior gives no indication that this lipid would favor the disordered phase; in fact, the opposite would be predicted. One possibility for this behavior may be attributed to the hydrophobicity of the cap spacer. In a lipid bilayer the hydrophobic spacer would attempt to minimize unfavorable interactions with water resulting in tight association to hydrophobic regions of the membrane (Figure 6). Strong association of the cap spacer with the bilayer would thus favor the disordered regions of the membrane. Studies by Sarmento et al.[19] provide further support for this idea when they showed that removal of the cap spacer can change the K_p from 0.26 for DPPE-cap-biotin to 1.1 for DPPE-biotin. These results suggest that the hydrophobic nature of the spacer plays a significant role in directing the lipid to less ordered regions of the membrane. The chemical structure of PEG offers a unique combination that promotes solvation in the aqueous phase with minimal inter- and intra-molecular interactions that can complicate recognition events.

We note a general trend of our lipids that with increasing length of the PEG spacers an enhanced partitioning towards the L_o phase was observed for all membrane compositions (Table 2). We believe there are at least two contributing factors for this partitioning behavior. The first factor relates to the host-guest interaction between the membrane and streptavidin. X-ray crystal structure[40] and electron spin resonance (ESR) studies[49] have determined streptavidin's binding pocket for biotin at approximately 8Å from the membrane surface. We estimate for the EG3 and EG5 spacers a maximum extension of the biotin group at ~3Å and ~10Å, respectively. As such, streptavidin interaction with these lipids may require some reorganization of the membrane structure. It can be argued that such displacements would preferentially occur on the disordered phase of the membrane thus resulting in lower values of K_p. In comparison, the longer PEG spacers of EG10 and EG15 (28Å and 46Å long tethers, respectively) provide ample distance for biotin-streptavidin interaction with minimal disruption of membrane. The second factor concerns the solvation of the biotin headgroup in the aqueous environment. Biotin has an octanol:water partition coefficient (log $P_{o/w}$) of 0.39,[50] indicating slight hydrophobicity. PEG spacers can provide a medium to assist solvation of biotin into the bulk solution and minimize strong association with the hydrophobic regions of the membrane. From our results the decamer and pentamer of PEG appear to have sufficient length to buffer the biotin-membrane interaction. This ability of the PEG spacer to decouple protein-membrane and headgroup-membrane interactions is key in lipid design thus enabling the preferred packing order defined by lipid tail structure to direct phase partitioning behavior.

Spacer volume also plays an important role in the partitioning of lipids (Figure 6). As discussed above, a minimal threshold of spacer length is required to 1) facilitate the biotin-streptavidin interaction and 2) decouple the biotin-membrane interaction. PEG2000 has the

length to achieve both goals, but its steric size could be a detriment to phase partitioning, as suggested by the K_p data. Based on its Flory radius, PEG2000 takes up a sizable area allowing only a few percent to reside within a domain. By shortening the PEG spacer to EG15 and EG10 we noted that K_p values increased as a result of reducing the spacer volume and allowing a higher concentration of biotinylated lipid in the L_o domain. Thus, for lipids with large spacers, high K_p values can be achieved by simply lowering its mole fraction in the membrane. It must be kept in mind, however, that the spacer size inversely correlates with the protein or probe density attainable within the membrane domain.

We also observed that with the PEG2000 spacer the biotinylated lipid tends to prefer less ordered versions of the L_o phase (i.e., lower T_{MT} membrane compositions). In some instances we even find that the phase to which FITC-streptavidin is bound is difficult to distinguish from the L_d phase. This difference in selectivity between large and small PEG spacers for low to high packing order in the L_o phase could serve as an additional tool for lipid design of phase selectivity in cell and model membranes.

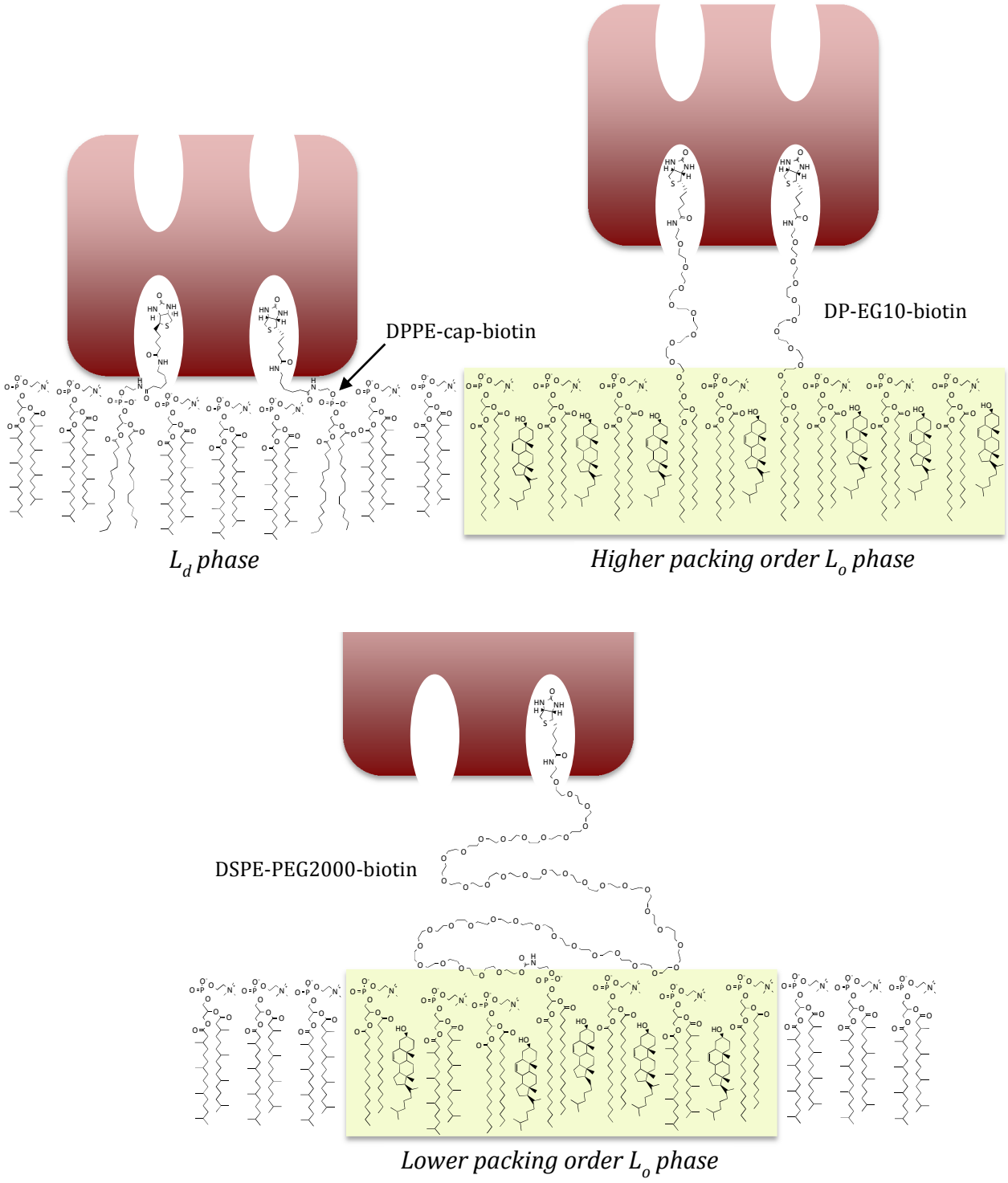

Figure 6. Schematic illustration of partitioning behavior of streptavidin bound biotinylated lipids into L_d and L_o phases. (Top left) DPPE-cap-biotin partitions into the L_d phase due to hydrophobic interaction of spacer and headgroup with membrane, (top right) DP-EG10-biotin with a sterically small but hydrophilic PEG spacer with selective partitioning into the L_o phase of high packing order, and (bottom) disruption of surrounding membrane order from bulky PEG spacer of DSPE-PEG2000-biotin.

Conclusions

Our results show that lipids can be rationally designed to partition to specific membrane phases. While preferred packing order dictated by lipid tail structure has typically been expected to determine phase partitioning, we found that spacer chemistry and size as well as headgroup hydrophobicity play influential roles. To allow the lipid tails to direct phase miscibility it is essential to decouple interactions of the spacer, headgroup, and host-guest interaction (e.g., protein binding) from the membrane. For the slightly hydrophobic biotin, using a hydrophilic PEG spacer can provide a medium to mitigate interactions with the membrane. Spacer length plays a role in mediating membrane-headgroup interaction and in the proper presentation of biotin for streptavidin binding. However, steric size of the spacer can negatively influence K_p and the structure of the ordered membrane phase. Our results demonstrated that for biotin-streptavidin interactions on the membrane surface EG10 and EG15 spacers provided optimal properties to allow strong partitioning for the L_o phase both in GUVs and GPMVs as directed by the palmityl tails of the lipids. Further investigation of the generality of this approach for lipid design to label domain architectures with probes and ligands are currently underway.

Acknowledgements

The authors would like to thank Ms April Nissen for conducting the DSC measurements on the lipids and Prof. Paul Cremer (Pennsylvania State University) and Profs. Marjorie Longo and Tonya Kuhl (UC Davis) for their insightful discussions. This work was supported by the US Department of Energy, Office of Basic Energy Sciences, Materials Science and Engineering Division (KC0203010). GPMV studies were performed by JCS, AG, and DJB under funding

from the National Science Foundation, Division of Materials Research under grant DMR-1352487. Sandia National Laboratories is a multi-program laboratory managed and operated by Sandia Corporation, a wholly owned subsidiary of Lockheed Martin Corporation, for the U.S. Department of Energy's National Nuclear Security Administration under contract DE-AC04-94AL85000.

¶ Current address: Department of Bioengineering, 205 Stanley Hall #1762, University of California, Berkeley, Berkeley, CA 94720

* Corresponding author, email: dysasak@sandia.gov

Supporting Information Available: Images and graphs of DSC measurements, Langmuir monolayer isotherms, and partitioning behavior of the biotinylated lipids in GUVs are shown here. This material is available free of charge via the Internet at http://pubs.acs.org.

References

1) A. J. Laude and I. A. Prior, *Molec. Membr. Biol.* 2004, **21**, 193-205.

2) K. Simons and D. Toomre, *Mol. Cell Biol.* 2000, **1**, 31-39.

3) M. F. Hanzal-Bayer and J. F. Hancock, *FEBS Lett.* 2007, **581**, 2098-2104.

4) S. Mañes, G. del Real, C. Martinez-A, *Nat. Rev. Immunol.* 2003, **3**, 557-568.

5) I. Levantal, M. Grzybek, K. Simons, *Biochemistry* 2010, **49**, 6305-6316.

6) R. M. Epand, *Biochim. Biophys. Acta* 2008, **1778**, 1576-1582.

7) D. Lingwood and K. Simons, *Science* 2010, **327**, 46-50.

8) G. van Meer, D. R. Voelker, G. W. Feigenson, *Nature Reviews* 2008, **9**, 112-124.

9) L. Johannes and S. Mayor, *Cell* 2010, **142**, 507-510.

10) J. H. Hurley, E. Boura, L.-A. Carlson, B. Rözycki, *Cell* 2010, **143**, 875

11) A. S. Klymchenko and R. Kreder, *Chem. Biol.* 2014, **21**, 97-113.

12) P. Sengupta, A. Hammond, D. Holowka, B. Baird, *Biochim. Biophys. Acta* 2008, **1778**, 20-32.

13) T. Baumgart, G. Hunt, E. R. Farkas, W. W. Webb, G. W. Feigenson, *Biochim. Biophys. Acta* 2007, **1768**, 2182-2194.

14) A. R. Honerkamp-Smith, S. L. Veatch, S. L. Keller, *Biochim. Biophys. Acta* 2009, **1788**, 53-63.

15) M. Ahlers, W. Müller, A. Reichert, H. Ringsdorf, J. Venzmer, *Angew. Chem. Int. Ed.* 1990, **29**, 1269-1285.

16) A. Lundquist, S. B. Hansen, H. Nordström, U. H. Danielson, K. Edwards, *Anal. Biochem.* 2010, **405**, 153-159.

17) Y. Hu, K. Li, L. Wang, S. Yin, Z. Zhang, Y. Zhang, *J. Control. Release* 2010, **144**, 75-81.

18) K. Kato, C. Itoh, T. Yasukouchi, T. Nagamune, *Biotechnol. Prog.* 2004, **20**, 897-904.

19) M. J. Sarmento, M. Prieto, F. Fernandes, *Biochim. Biophys. Acta* 2012, **1818**, 2605-2615.

20) S. Manley, M. R. Horton, S. Lecszynski, A. P. Gast, *Biophys. J.* 2008, **95**, 2301-2307.

21) T.-Y. Wang, R. Leventis, J. R. Silvius, *J. Biol. Chem.* 2005, **280**, 22839-22846.

22) A. Honigmann, V. Mueller, S. W. Hell, C. Eggeling, *Farad. Discuss.* 2012, **161**, 77-89.

23) *Poly(ethylene glycol);* Harris, J. M.; Zalipsky, S., Eds.; ACS Symposium Series 680; American Chemical Society: Washington, DC, 1997.

24) A. R. Nicholas, M. J. Scott, N. I. Kennedy, M. N. Jones, *Biochim. Biophys. Acta* 2000, **1463**, 167-178.

25) T. L. Kuhl, J. Majewski, P. B. Howes, K. Kjaer, A. von Nahmen, K. Y. C. Lee, B. Ocko, J. N. Israelachvili, G. S. Smith, *J. Am. Chem. Soc.* 1999, **121**, 7682-7688.

26) J. Majewski, T. L. Kuhl, K. Kjaer, M. C. Gerstenberg, J. Als-Nielsen, J. N. Israelachvili, G. S. Smith, *J. Am. Chem. Soc.* 1998, **120**, 1469-1473.

27) M. A. Borden, G. V. Martinez, J. Ricker, N. Tsvetkova, M. L. Longo, R. J. Gillies, P. A. Dayton, K. W. Ferrara, *Langmuir* 2006, **22**, 4291-4297.

28) F. K. Bedu-Addo, P. Tang, Y. Xu, L. Huang, *Pharm. Res.* 1996, **13**, 710-717.

29) K. Edwards, M. Johnsson, G. Karlsson, M. Silvander, *Biophys. J.* 1997, **73**, 258-266.

30) D. A. Noppl-Simson and D. Needham, D. *Biophys. J.* 1996, **70**, 1391-1401.

31) C. Allen, N. Dos Santos, R. Gallagher, G. N. C. Chiu, Y. Shu, W. M. Li, S. A. Johnstone, A. S. Janoff, L. D. Mayer, M. S. Webb, M. B. Bally, *Biosci. Reports* 2002, **22**, 225-250.

32) J. C. Stachowiak, C. C. Hayden, M. A. A. Sanchez, J. Wang, B. C. Bunker, J. Voigt, D. Y. Sasaki, *Langmuir* 2011, **27**, 1457-1462.

33) J. A. Last, T. A. Waggoner, D. Y. Sasaki, *Biophy. J.* 2001, **81**, 2737-2742.

34) M. I. Angelova and D. S. Dimitrov, *Farad. Discuss. Chem. Soc.* 1986, **81**, 303-311.

35) E. Sezgin, H.-J. Kaiser, T. Baumgart, P. Schwille, K. Simons, I. Levental, *Nat. Protocols* 2012, **7**, 1042-1051.

36) T. Baumgart, A. T. Hammond, P. Sengupta, S. T. Hess, D. A. Holowka, B. A. Baird, W. W. Webb, *Proc. Natl. Acad. Sci. USA* 2007, **104**, 3165-3170.

37) T. R. Baekmark, G. Elender, D. D. Lasic, E. Sackmann, *Langmuir* 1995, **11**, 3975-3987.

38) D. Marsh, *Biochim. Biophys. Acta* 1996, **1286**, 183-223.

39) S. L.Veatch, K. Gawrisch, S. L. Keller, *Biophys. J.* 2006, **90**, 4428-4436.

40) S. A. Darst, M. Ahlers, P. H. Meller, E. W. Kubalek, R. Blankenburg, H. O. Ribi, H. Ringsdorf, R. D. Kornberg, *Biophys. J.* 1991, **59**, 387-396.

41) R. D. Kornberg and S. A. Darst, *Curr. Opin. Struct. Biol.* 1991, **1**, 642-646.

42) C.-H. Hsieh, S.-C. Sue, P.-C. Lyu, W.-g. Wu, *Biophys. J.* 1997, **73**, 870-877.

43) J. C. Stachowiak, C. C. Hayden, D. Y. Sasaki, *Proc. Natl. Acad. Sci. USA* 2010, **107**, 7781-7786.

44) C. S. Scheve, P. A. Gonzales, N. Momin, J. C. Stachowiak, *J. Am. Chem. Soc.* 2013, **135**, 1185-1188.

45) O. Edholm and J. F. Nagle, *Biophys. J.* 2005, **89**, 1827-1832.

46) V. Tsukanova, C. Salesse, *J. Phys. Chem. B* 2004, **108**, 10754-10764).

47) P. G. de Gennes, *Macromolecules* 1980, **13**, 1069-1075.

48) T.-H. Chou and I.-M. Chu, *Coll. Surf. A: Physiochem. Eng. Aspects* 2002, **211**, 267-274.

49) M. J. Swamy and D. Marsh, *Biochemistry* 1997, **36**, 7403-7407.

50) Octanol/water partition coefficients can be found at the U.S. National Library of Medicine Toxicology Data Network. http://www.toxnet.nlm.nih.gov